

# 1

## Tools for Doing Nuclear Physics

“Science clears the fields on which technology can build.”

—Werner Heisenberg

### PART-I: PHYSICAL TOOLS

#### ■ 1.1.1 INTRODUCTION

Imagine the plight of a hiker on hills not having a can-opener or knife to open cans of food. It is a terrible experience to be stranded without proper tools. In understanding nuclear physics also we need tools. During the past 100 years, many ingenious and powerful tools have been invented. Some of them have no longer remained part of nuclear exploration alone, but have acquired wide applications in fields like chemistry, biochemistry, biophysics, atomic and molecular physics and so on. For example, the technique of Nuclear Magnetic Resonance (NMR), which has its origin in Nuclear Physics, is increasingly being used in areas other than Nuclear Physics. In Chapter 9 we will consider some techniques of Nuclear Physics widely used in other areas of science.

It is equally important to learn the skills of using some mathematical tools, particularly some elementary wave mechanics, without which it is impossible to appreciate and understand Nuclear Phenomena. To familiarise the students with these tools, this chapter has been divided into two parts. Part I deals with Physical Tools like nuclear radiation detectors, accelerators, spectrometers, etc. On the other hand, Part II deals with Mathematical Tools like wave mechanics of a particle in a potential barrier or well. Both these parts deal with basic tools essential to the understanding of Nuclear Physics.

## 1.I.2 INTERACTION BETWEEN PARTICLES AND MATTER: A BRIEF SURVEY

The design of a nuclear radiation detector depends on our understanding of passage of radiation through matter. Strictly, this is governed by Atomic Physics. However, because of its importance in the design of nuclear detectors, we shall outline its main features.

When a collimated beam of monoenergetic particles passes through a piece of matter, there are two extreme cases of interest: (i) In the first case, a particle undergoes many interactions, every time losing a small amount of energy and suffering a small-angle scattering; (ii) In the second case the particle either passes unharmed through the material or is removed from the beam in one single 'catastrophic' encounter. These two cases are depicted in Figs. 1.I.1 (a) and (b).

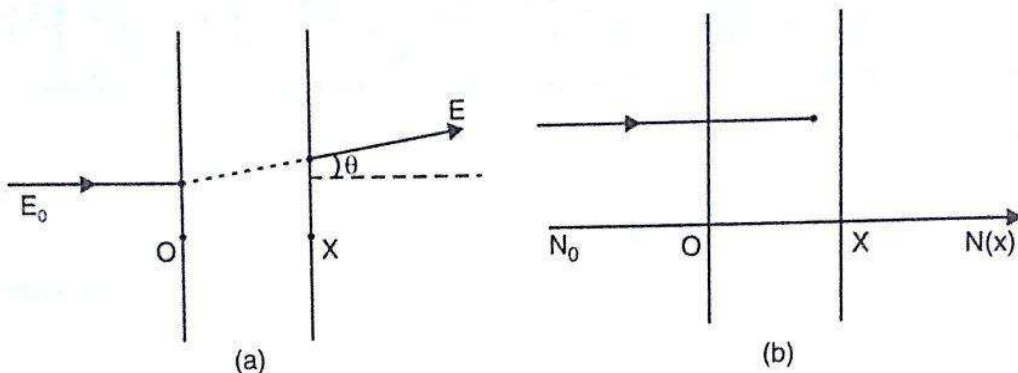


**Fig. 1.I.1.** Passage of a collimated beam of particles through matter.

- (a) Each particle undergoes many interactions.
- (b) A particle is either removed from the beam or passes unharmed.

We shall consider these two cases in some detail.

(i) When a particle undergoes many interactions, it progressively loses energy. A monoenergetic beam of such particles will show an energy spread as shown in Fig. 1.I.2.

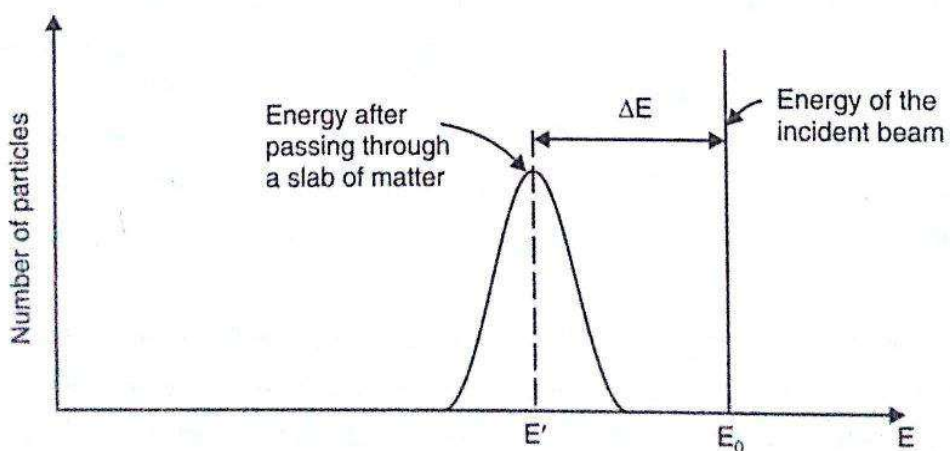


**Fig. 1.I.2.** Energy spread of a beam of monoenergetic, heavy and charged particles after passing through a slab of matter.

Figure 1.I.3 shows the behaviour of a number of particles transmitted through an absorbing piece of matter as a function of the absorber thickness.

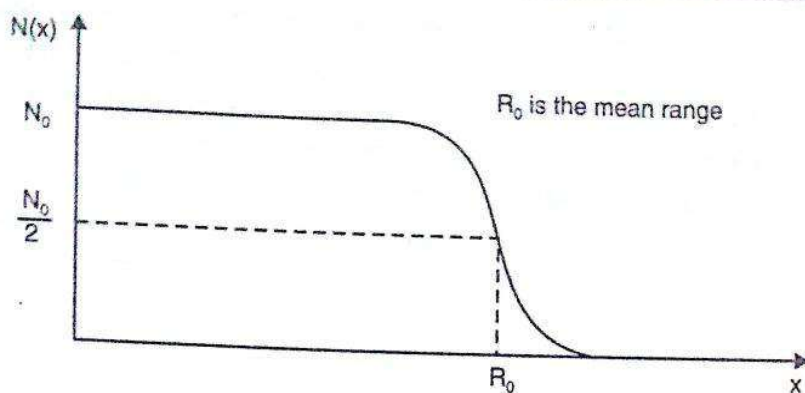


Fig. 1.I.3. Existence of range for a beam of heavy charged particles.

Clearly, all particles are transmitted up to a certain thickness. At a thickness  $R_0$ , half the particles get stopped.  $R_0$  is the *mean range*. At a sufficiently large thickness, all particles get stopped. The fluctuation in range is called *straggling*.

Heavy charged particles like a proton,  $\alpha$ -particle, fission fragment, etc. fall in this category. They all have a fairly definite *range* in a gas, liquid or solid. We repeat that the energy loss occurs in a large number of small interactions. The particle has such a large momentum that its direction is not significantly changed during its slowing process (see Fig. 1.I.1). The energy loss is mainly due to the excitation and ionisation of atoms in its path. These heavy charged particles lose more energy per unit length of the path near the end of their range, since they are moving more slowly and have more time to interact with the atoms which they pass by. This enables us to assume that the energy loss per unit length of the path is inversely proportional to the velocity,  $v$ .

$$\therefore \frac{-dK}{dx} = \frac{C}{v}$$

where  $C$  is a constant that depends on the absorbing material. For heavy charged particles like an  $\alpha$ -particle, we can say:  $K = \frac{1}{2}mv^2$  = kinetic energy.

$$\therefore -mv \frac{dv}{dx} = \frac{C}{v}$$

Let  $R$  be the range of the particle. Therefore, for  $x = 0$ ,  $v = v_0$  and for  $x = R$ ,  $v = 0$ . Separating the variables we have,

$$\int_{v_0}^0 -mv^2 dv = \int_0^R C dx$$

$$\frac{mv_0^3}{3} = CR$$

This gives,

$$v_0^3 = C'R \quad \dots(1.I.1)$$

or

$$v_0^3 = C'R$$

where  $C'$  is another constant depending on the absorbing material. Equation 1.I.1 is *Geiger's rule*. This rule is approximately correct for any charged, heavy particle in any medium and explains how the range  $R$  is related to the particle's energy. The measurement of the range of a heavy charged particle is a common method for measuring its energy. Figure 1.I.4 shows the ranges of  $\alpha$ -particles and protons in air. Notice that the range of  $\alpha$ -particle is much shorter than that of a proton with the same energy. This is because the  $\alpha$ -particle is slower and is more charged than the proton with the same energy and so, is more ionising.

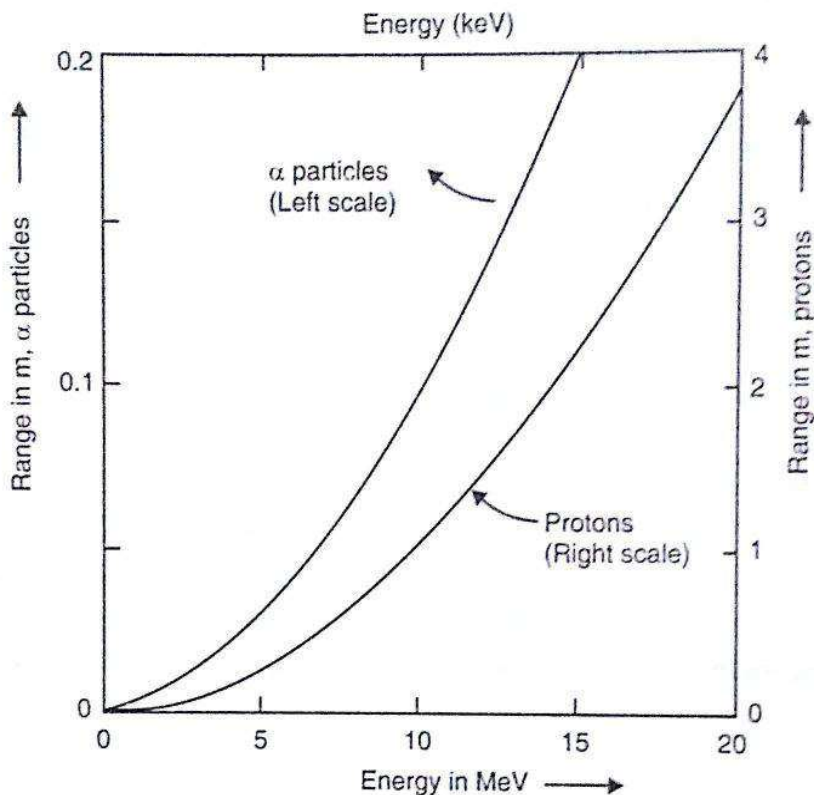


Fig 1.I.4. Ranges of  $\alpha$ -particles and protons in air at  $15^\circ\text{C}$  and  $76 \text{ cm Hg}$  pressure. [From *Experimental Nuclear Physics*, Vol. I, E. Segre, ed., Wiley (1953)].

The energy loss rate –  $-dK/dx$  is called the *stopping power*. It varies from substance to substance because the atomic levels are different and so the energy loss in the ionisation process varies. A more significant factor affecting the stopping factor is the density of the absorber as the number of electrons in a unit volume is roughly proportional to the density. The more the number of electrons per unit volume, the more is the energy loss due to the excitation of these

electrons. If we replace  $-dK/dx$  by  $-\left(\frac{1}{\rho}\right)\frac{dK}{dx}$  where  $\rho$  is the density, the stopping powers

(now expressed in  $\text{kg per m}^2$  of matter traversed) become comparable. For example, the range of 10 MeV protons is about  $1.4 \text{ kg m}^{-2}$  in air,  $1.7 \text{ kg m}^{-2}$  in aluminium and  $2.1 \text{ kg m}^{-2}$  in copper.

(ii) Let us now consider the second important case of interaction between a monoenergetic beam of particles and matter in such a manner that a particle in the beam is either unharmed in the absorber or is totally removed from the beam in a single "catastrophic" event (see Fig. 1.I.1).

If an interaction removes the particle from the beam then the features of the transmitted beam are quite different from those described before. Clearly, the transmitted beam has the

same particle energy because those particles which have come out of the absorber (or are transmitted) have not undergone any interaction. For every material thickness  $dx$ , the number of particles undergoing interactions is proportional to the number of incident particles and so.

$$-\frac{dN}{dx} = \mu N(x)$$

where  $\mu$  is the constant of proportionality called the *absorption coefficient*. This on integration yields.

$$N(x) = N_0 e^{-\mu x} \quad \dots(1.1.2)$$

i.e., the number of transmitted particles decreases exponentially. This is indicated in Fig. 1.1.5.

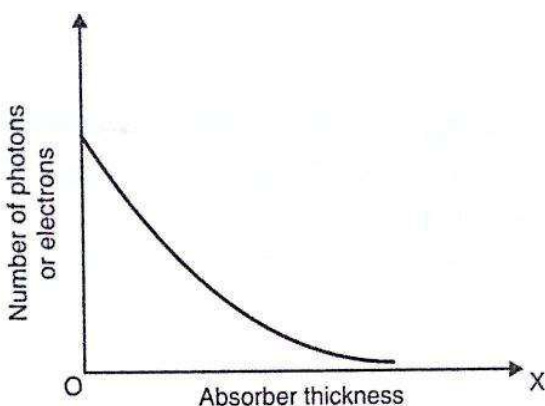


Fig. 1.1.5. Absorption of light particles like photons or electrons by matter.

In this case, no range can be defined, but one can talk about the mean free path defined as the average distance travelled by a particle before undergoing a collision. This mean free path is equal to  $1/\mu$ . Photons or electrons approximate this behaviour.

The slowing down of electrons with energies less than 1 MeV is like the slowing down of heavy charged particles. This is mainly due to the ionisation and excitation-collision processes. However, the electron does not exhibit a well-defined range because (i) it is much lighter than the proton (the mass of electron is  $1/1836$  the mass of proton) and so can be easily deflected from the direction of the main beam; and (ii) a few collisions are sufficient to stop an electron. At higher energies ( $K.E. > 1$  MeV), the energy loss of an electron is chiefly due to *Bremsstrahlung* (production of continuous X-rays). The probability for this process increases with the energy.

Figure 1.1.6 depicts the Bremsstrahlung process.

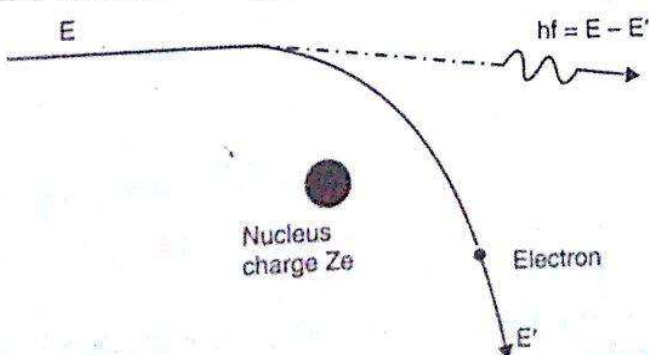


Fig. 1.1.6. The accelerated electron radiates and loses energy in the form of a photon (Bremsstrahlung).

We shall now outline the interaction between photons and matter. Photons interact with matter through three principal processes.

1. Photoelectric effect
2. Compton effect
3. Pair production.

In the photoelectric effect, an atom absorbs the photon and an electron from one of the shells is ejected. In the Compton effect, the photon gets scattered by an atomic electron. In pair production, the photon is converted into an electron positron pair. This last process can occur only in the presence of the nuclear Coulomb field which helps to balance energy and momentum.

The likelihood of the above three processes is energy dependent. At low energies below a few keV the photoelectric effect dominates, the Compton effect is negligible and pair production is energetically impossible.

The rest energy  $2 m_0 c^2$  of the pair is 1.02 MeV, and so the  $\gamma$ -ray must have at least an energy of 1.02 MeV to produce a pair. If the energy of the incident  $\gamma$ -ray is 3.02 MeV, for example, the electron and positron would share 2.00 MeV of kinetic energy. If this kinetic energy can be measured, it would tell us the  $\gamma$ -ray energy.

Equation 1.I.2 is also valid for  $\gamma$ -ray absorption (like for electron absorption).

Recall that this equation is a direct consequence of the fact that photons do not lose energy in small steps; a photon is either scattered out of the beam or is absorbed. The attenuation of a monochromatic beam of photons follows Eq. 1.I.2.

The absorption constant  $\mu$  for  $\gamma$  photons of various energies is illustrated in Fig. 1.I.7.

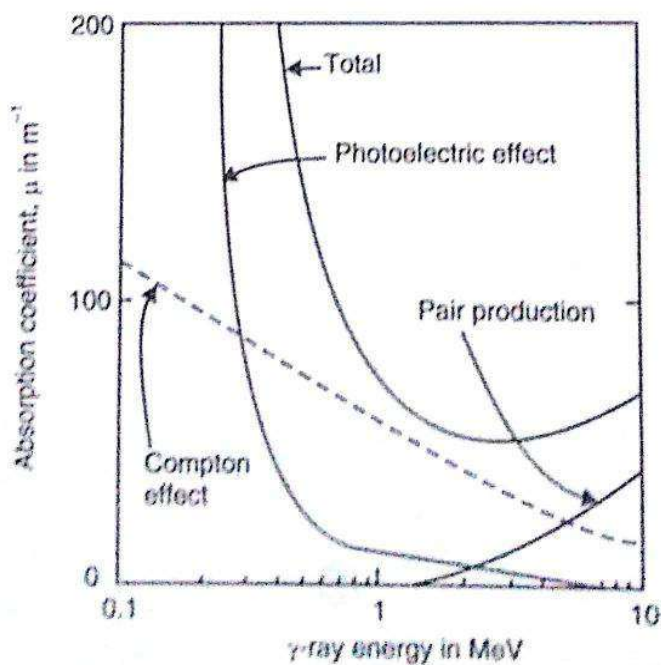


**Fig. 1.I.7.** Absorption of  $\gamma$ -rays in lead. The 'total' curve is obtained by adding the  $\mu$  for the 3 important processes. (From W. Heitler, *The Quantum Theory of Radiation*, 3rd Ed., Clarendon Press, Oxford, 1954.)

### 1.1.3 DETECTORS FOR NUCLEAR PARTICLES

The survey of interaction between particles and matter would help us in understanding features of detectors for nuclear particles. It will be impossible to describe all the different types of detectors in this small section and so, we will stick to some widely and currently used instruments. Ionisation produced by charged particles is the basis for detecting many nuclear particles. In gases, one electron-ion pair is formed for each 30 eV of energy lost by the charged particle. The  $\alpha$ -particles and protons, lose energy rapidly by ionisation, and so such particles lose all their energy in the detector. On the other hand, electrons and photons ( $\gamma$ -rays) lose only a fraction of their original energy in a gas-filled detector. Because of its high penetrating power, the  $\gamma$ -ray is particularly difficult to detect.

#### (i) Proportional Counter

A schematic sketch of the proportional counter is shown in Fig. 1.1.8. It is a metal chamber filled with a gas and having a thin wire (diameter  $\sim 0.1$  mm) axially along the centre. This wire is made anode, by connecting it to a power supply as shown in the figure. A voltage of a few hundred volts which does not cause a discharge is applied between the wire anode and the metal case, which acts as the cathode. Consider now the entry of an ionising particle into the chamber through the thin mica "end window". Electrons produced are attracted toward the central wire anode. The electric field in the vicinity of the fine wire is very large compared to the other regions in the chamber and as a result, an electron near the wire acquires enough energy between two successive collisions with the gas atoms to enable it to ionise gas atoms. This produces additional ion pairs (electrons and positive ions). This process is called gas amplification and the number of ions increases by a factor  $\sim 10^4$ .

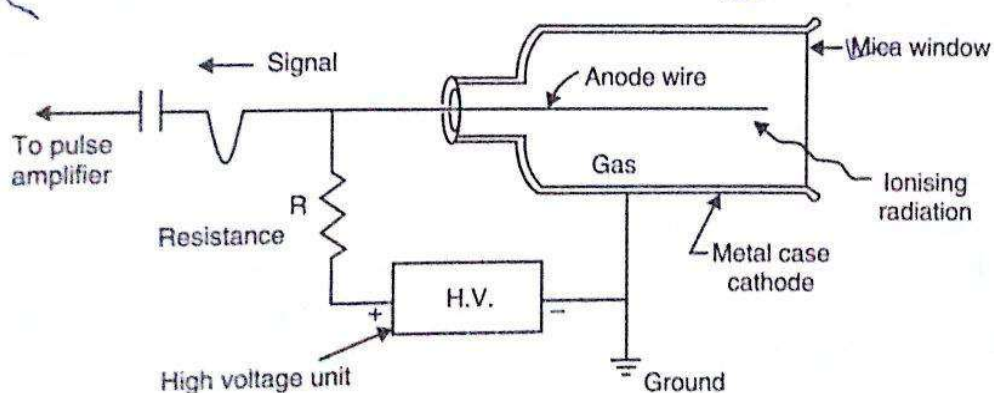


Fig. 1.1.8. 'End window' type proportional counter.

The important fact is that the output pulse of the current is proportional to the number of initial ion pairs produced by the ionising particle entering the chamber. That is, the output signal is proportional to the energy of the incident particle. Because of the IR drop across the resistance, the current pulse produces a voltage pulse, which is amplified and recorded.

When a  $\gamma$ -photon enters the chamber, the ionisation occurs mainly due to the emission of electrons from the counter walls. Due to the large penetrating power of gamma rays a  $\gamma$ -ray photon is less likely to produce direct ionisation of gas atoms.

*output signal  $\propto$  energy of incident particle*

Usually the gas used is a pure noble gas, because electrons then remain free and can be rapidly collected. For counting fast neutrons, a gas containing hydrogen can be used. Due to elastic collisions, protons are produced and can be detected. When slow neutrons are to be counted, the counter can be filled with the gas  $\text{BF}_3$ . The following reaction takes place:



The  ${}^7_3 \text{Li}$  and  ${}^4_2 \text{He}$  atoms move very rapidly and so their electrons are stripped off as they pass through the gas.

## (ii) The Geiger Counter - T.Y. Book

The construction of the Geiger Counter is similar to that of the proportional counter (see Fig. 1.1.8). However, the voltage applied to the Geiger Counter is large enough, so that even a single ion pair produced by a single incident particle can produce an electric discharge. Usually, a voltage of about 1000 volts or so for a typical pressure of about 100 mm of mercury is enough to trigger off a discharge when an incident particle enters the Geiger Counter. The important thing is that the electric pulse produced in this discharge is the same, whatever the energy of the incident particle.

The anode wire is surrounded by the slow moving positive ion sheath, which reduces the electric field, making the discharge stop within a few microseconds ( $10^{-6}$  s). As the positive ion sheath moves away from the anode wire towards the tube's wall (cathode), the value of the electric field rises to permit another electric discharge due to production of electrons when the positive ions hit the wall of the tube. This results in a continuous electric discharge and the tube is not ready to receive another incident particle. Therefore, some mechanism must be devised to terminate the discharge after each event (Quenching of the counter).

The simplest method for achieving this is to make the resistor  $R$  very large ( $\sim 10^6$  ohms). For a large current (at the time of discharge), this resistance has a large voltage drop (IR drop) which makes the potential difference between the anode and cathode fall off to such an extent that the discharge in the counter cannot be maintained. However, this has the effect of prolonging the time before the counter can become ready to accept another pulse. This time interval is called the dead time and is of the order of  $200 \mu\text{sec}$ .

The monoatomic argon, which is transparent to ultraviolet light, is usually used in the Geiger Counters at a pressure of about 100 mm of mercury. It is possible to make these counters self-quenching by mixing argon with a polyatomic molecule such as alcohol. Typically, a Geiger Counter contains about 10 per cent alcohol and 90 per cent argon. This has the effect of ultraviolet photons from the argon getting absorbed by the alcohol so that they do not reach the cathode. Now, as the positive ions move toward the cathode, they collide with alcohol molecules resulting in the transfer of an electron from the alcohol molecule to the argon, neutralising it.

The alcohol molecules, upon arrival at the cathode, dissociate rather than eject electrons so that the discharge gets quenched. Such self-quenching by organic molecules results in the dissociation of molecules and after about  $10^9$  discharges, these molecules are used up necessitating refilling.

*An Electric pulse is independent of the particle's Energy.*

of the Geiger Counter. It is possible to use halogen molecules for quenching, their advantage being their tendency to recombine after dissociation.

In conclusion, one can say that the Geiger Counter is a very sensitive device for detecting charged particles and it produces a large pulse requiring no amplification. It suffers from the disadvantages of being quite slow, being incapable of providing information about the type of particle which may have produced a count and its lack of information about the energy of the particle counted.

### (iii) Scintillation Counter

One of the early methods used for the detection and counting of  $\alpha$ -particles was to make them strike a zinc sulphide screen and then observe the scintillations on the screen through a lens acting as a magnifier. The modern scintillation counter uses a scintillating crystal. Light from the crystal is incident on a photosensitive surface called the photo cathode of a photomultiplier tube. Photoelectrons produced at this photocathode are directed by an appropriate accelerating voltage to the first dynode (anode), where a single accelerated photoelectron can knock out "secondary"

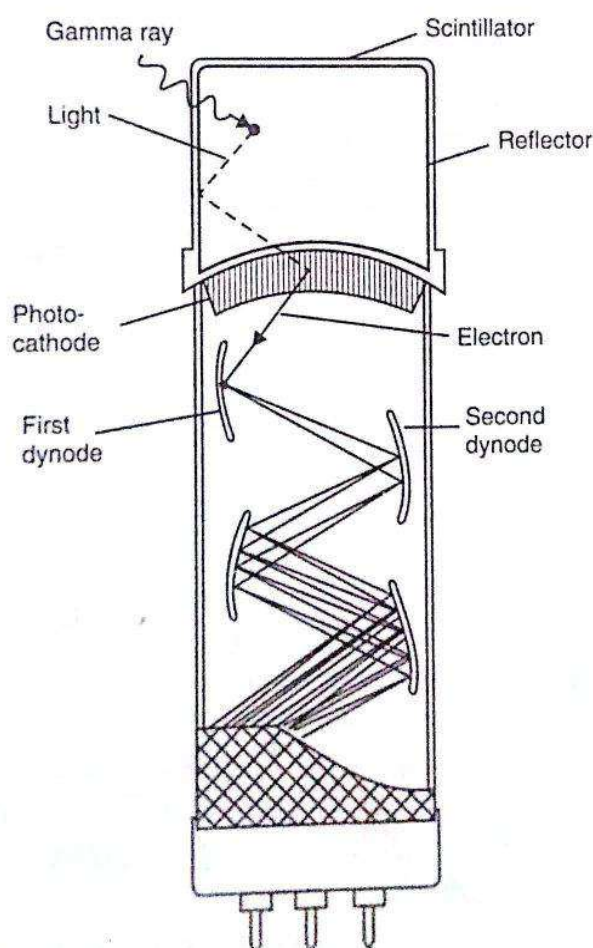
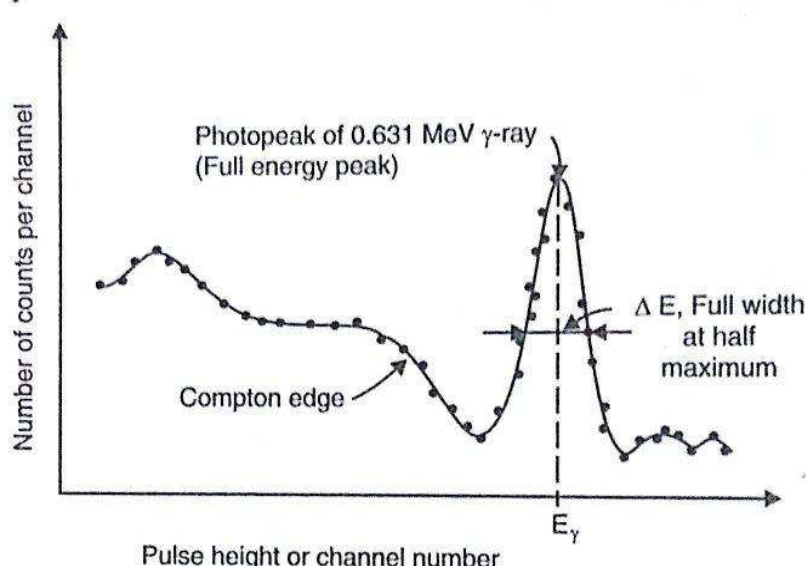


Fig. 1.1.9. Scintillator put on a photomultiplier tube. An overall multiplying factor of up to  $10^9$  can be achieved.

electrons. This dynode is the cathode relative to another dynode where more secondary electrons are liberated. This process continues through several stages (about 10 to 14) until the burst of

electrons becomes large enough to constitute an electric pulse that can be further amplified by an electronic amplifier. Pulses from this amplifier are then electronically counted. By this technique individual radiation particles of very low energy can also be counted. Figure 1.1.9 shows a scintillator mounted on a photomultiplier tube. The most important property of such an assembly is that [the electric pulses produced are proportional to the energy of the incident  $\gamma$ -rays]. Thus it is possible not only to detect the  $\gamma$ -rays but to measure their energy as well. A specialised computer like device called a multichannel analyser can sort out the output-electric pulses according to their magnitudes and record the number of pulses of each magnitude entering the instrument. The resulting data constitutes an energy spectrum of the  $\gamma$ -rays penetrating the scintillator crystal.

A typical  $\gamma$ -ray spectrum obtained with  $^{137}\text{Cs}$  source is shown in Fig. 1.1.10.



**Fig. 1.1.10.**  $\gamma$ -ray spectrum of  $^{137}\text{Cs}$ . The single photoelectric peak of 0.631 MeV  $\gamma$ -ray follows the Compton edge.

$\gamma$ -ray being energetic photons (uncharged) have to be indirectly detected. As seen in the previous section,  $\gamma$ -rays interact with matter mainly in three ways: the photoelectric effect, the Compton effect and the production of the positron-electron pair. [For  $\gamma$ -ray having an energy of up to 2 MeV, the first two processes are the most important, but it is the photoelectric effect which is actually utilised.] This is because when a  $\gamma$ -ray produces a photoelectron, the photoelectron has an energy which is essentially the same as the absorbed  $\gamma$ -ray energy. In the photoelectric effect, the  $\gamma$ -ray loses all its energy. [Thus all  $\gamma$ -ray of one energy will produce in a scintillating crystal, photoelectrons having the same energy.] The amount of light produced in the crystal being proportional to this energy, the electrical pulse obtained from the photomultiplier will also be proportional to the  $\gamma$ -ray energy.

Two types of scintillators are widely used: sodium iodide and plastic. Sodium iodide crystals are usually doped with a small amount of thallium and denoted by NaI(Tl). The Tl atoms act as luminescence centres. NaI(Tl) crystals are dense enough to have good efficiency of  $\gamma$ -ray detection but the decay of each pulse is slow ( $\sim 0.25 \mu\text{sec}$ ) compared to plastic which has a decay time of  $\sim 10^{-9} \text{ sec}$ . However, the  $\gamma$ -ray collection efficiency of plastic is low and so they are mainly used for the detection of charged particles like electrons.

Look at Fig. 1.1.10. The Compton electrons may have any value from zero up to the maximum, which is about 0.22 MeV less than the  $\gamma$ -ray energy (in the energy range of 0.5 MeV to 5 MeV). The Compton electrons are spread out more or less continuously under the photopeak and form a 'background'. The *Compton 'edge'* representing the maximum energy Compton electrons, can be clearly seen in Fig. 1.1.10. The pair production effect is useful for detecting higher energy  $\gamma$ -ray.

A scintillation counter coupled with a multichannel analyser constitutes a  $\gamma$ -ray spectrometer. Such a  $\gamma$ -ray spectrometer must be calibrated using  $\gamma$ -ray of known energy. The width of the full energy peak at half height is called *full width at half maximum, FWHM*. It depends on the number of light photons produced by the incident  $\gamma$ -ray photon. Typically  $\frac{\Delta E}{E_\gamma}$  is of the order of 20 per cent at  $E_\gamma = 100$  keV and 6 to 8 per cent at  $E_\gamma = 1$  MeV (for the NaI detector).

$$\frac{\Delta E}{E_\gamma} = \text{energy resolution.}$$

In many cases, a resolution of about 10 per cent is sufficient. However, [in some cases  $\gamma$ -ray energies are so close that a scintillation counter is unable to separate them. One has to then use a semiconductor detector.]

#### (iv) Solid State or Semiconductor Detectors

Before discussing the semiconductor detector, it will be of interest to compare a gamma ray spectrum as seen by a semiconductor detector and by a scintillation detector. Figure 1.1.11 shows the  $\gamma$ -ray spectrum of  $^{60}\text{Co}$  (cobalt-60) observed by a germanium detector and a scintillation detector.

The tremendous improvement in energy resolution provided by the solid state, Lithium Drifted Germanium (Ge(Li)) detector has brought these detectors to the forefront since 1960 and in many areas, they have completely replaced scintillation counters.

A solid state detector, like an ionisation chamber, collects and measures the charge liberated by incident radiation. However, it has *two* great advantages over an ionisation chamber using a gas: (i) Because of the greater density of solids.

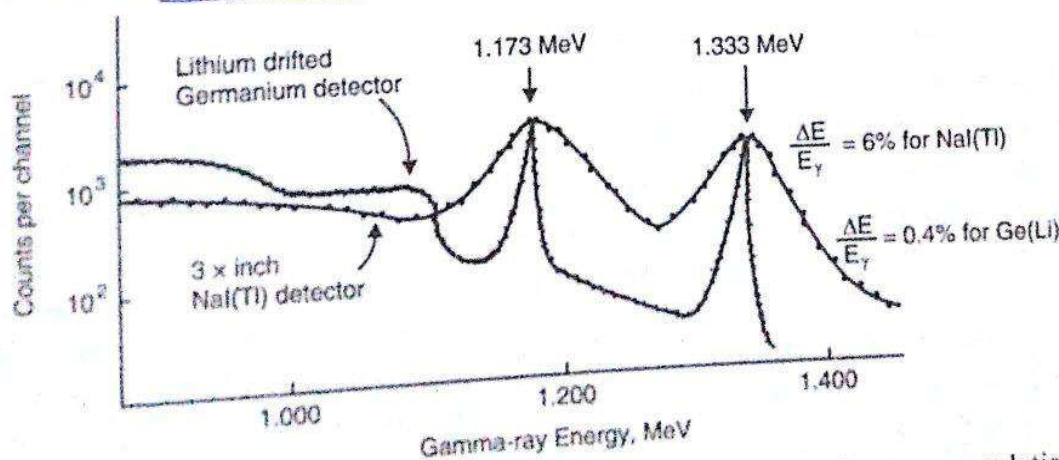
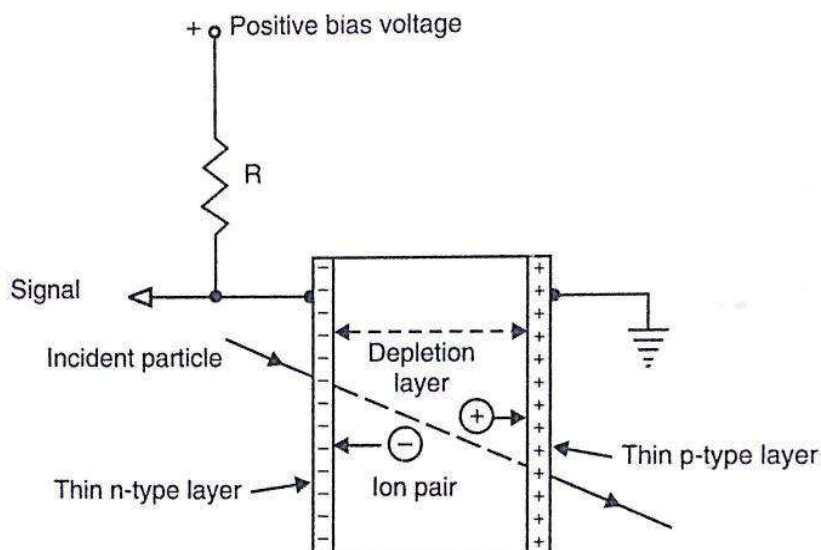


Fig. 1.1.11. Gamma ray spectrum of  $^{60}\text{Co}$ . Note the fantastic improvement in energy resolution provided by Ge(Li), (Lithium drifted Germanium detector) compared to NaI(Tl) scintillation detector.

compared to gases they have much greater stopping power for incident radiation. This implies that even for penetrating radiation like  $\gamma$ -ray, a solid state detector can be used. (ii) The energy required for the production of an ion pair in solids is much lower than in gases. Let this energy be  $W$ .  $W = 42 \text{ eV}$  for helium,  $22 \text{ eV}$  for xenon and  $34 \text{ eV}$  for air. On the other hand,  $W = 2.9 \text{ eV}$  for germanium and  $3.5 \text{ eV}$  for silicon. The energies are low for these solids because ionisation does not occur from an atomic level to the continuum, but from the valence band to the conduction band. Lower values of  $W$  imply higher energy resolution, as is clear from Fig. 1.I.11.

A semiconductor detector is actually a reverse biased p-n junction. It is schematically shown in Fig. 1.I.12.



**Fig. 1.I.12.** An ideal semiconductor detector, showing fully depleted region and thin heavily doped surface layers of opposite types.

When ionising radiation enters the depletion layer which is free from any charges, it produces hole-electron pairs. Because of the smaller value of  $W$  compared to gases we have many more ions produced, and hence the statistical fluctuation in the number of ions is much less, resulting in highly improved resolution.

With very pure semiconductor materials, depletion layers of only about 1 mm are attainable. This thickness is enough to stop an  $\alpha$ -particle or a proton, but not to stop a  $\gamma$ -ray photon. It was for this reason that an ingenious technique known as lithium drifting was developed.

Usually lithium is diffused into the surface of  $p$ -type germanium. The device is then heated ( $\sim 200^\circ \text{ C}$ ) to increase the mobility of lithium atoms and a reverse bias is applied. Positive lithium ions then *drift* into the depletion layer and *compensate the negative impurities* in the  $p$ -type region. Thus, this drift of Li-ions produces a very pure semiconductor region (with no charge carrier) between the  $n$  and  $p$ -type regions. Depletion layers of several centimetres (7 cm or more) have been produced in this manner, making the detector extremely useful for  $\gamma$ -ray detection as well.

Figure 1.I.13 shows the  $\gamma$ -ray spectrum of  $7.5 \text{ h}^{171}\text{Er}$  using a  $20 \text{ cm}^3$  Ge(Li) detector. The energy resolution is  $\sim 0.4$  per cent at 1 MeV. Ge(Li)-detectors having volumes up to  $100 \text{ cm}^3$

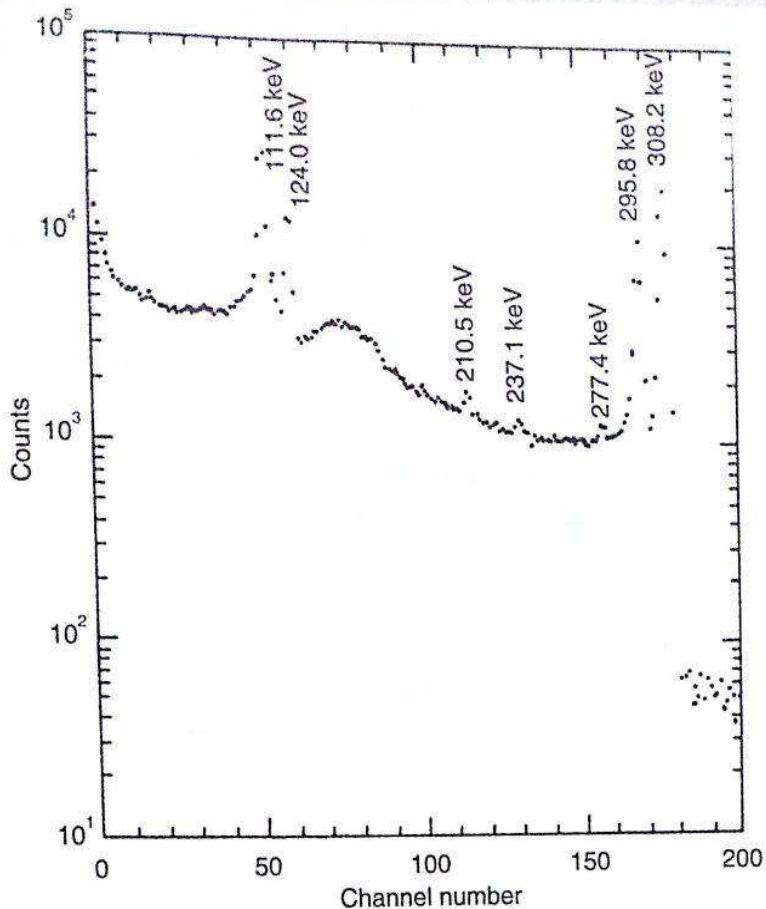


Fig. 1.I.13.  $\gamma$ -ray spectrum of 7.5 h  $^{171}\text{Er}$  using a  $20\text{ cm}^3$  Lithium Drifted Germanium, Ge(Li) detector. (S.B. Patel et al., *Phys., Rev. C*, Vol. 14 No. 5, 1976.)

have been routinely built. These are particularly useful in high energy physics. Germanium, because of its higher density as compared to silicon, is more suitable for  $\gamma$ -ray detection. However, it has disadvantage: It must be cooled since some hole-electron pairs can be produced by as little as 0.66 eV and at room temperature thermal energies are sufficient to produce such pairs. Ge(Li) detectors are thus thermally connected with a copper finger, the tip of which is always kept dipped into liquid nitrogen.

#### (v) Compton Suppressed Germanium Detectors

Two recent developments have taken the field of  $\gamma$ -ray spectroscopy by storm. The first is the development of intrinsic germanium detectors made from ultra pure germanium. Large enough depletion layers can be obtained without lithium drifting. Further a compact liquid nitrogen dewar arrangement makes it possible to use many detectors together for multiple coincidence work.

The second is the use of anti-Compton shields on the germanium detectors. This makes even the weakest  $\gamma$ -lines to stand out in the  $\gamma$ -spectrum.

These developments have revolutionised our tools for nuclear spectroscopy. Let us therefore look at this new  $\gamma$ -ray detector in some detail.

The primary criterion for a  $\gamma$ -ray detector is that every  $\gamma$ -ray that strikes the detector should result in a voltage pulse, proportional to the original  $\gamma$ -ray energy. Technically, one says that a detector must have a good response function. Unfortunately, a germanium detector does not

satisfy this requirement quite well. It has the atomic number  $Z = 32$ , which is relatively low. Germanium is also moderately dense and it interacts with  $\gamma$ -rays mainly by Compton scattering. For  $\gamma$ -rays in the energy range of about 1 MeV. With about a  $20 \text{ cm}^3$  Ge-detector, a 1 MeV  $\gamma$ -ray has an absorption probability of about  $3/4$ . This implies that  $1/4$  of such  $\gamma$ -rays do not interact at all with the detector. Further, out of those  $\gamma$ -rays which interact with the Ge-detector, only about 15 to 20 per cent give rise to useful full-energy peaks (photo-peaks). This is evident in Fig. 1.1.11. If the area under the  $\gamma$ -rays spectrum is measured, it gives the ratio:

$$\frac{\text{Area under photo-peak}}{\text{Total area}} = \frac{P}{T} \equiv 15 - 20\%$$

Thus about 80 to 85 per cent events in the Ge-detector do not correspond to full  $\gamma$ -ray energy, implying a poor response function. Consequently, these majority events (80–85 per cent) form unwanted garbage. This is the story of the  $\gamma$ -ray *singles spectrum*. Often one wants to determine a sequence of  $\gamma$ -rays and so a coincidence measurement has to be performed (see Sec. 1.1.6). Coincidence measurement involving 2  $\gamma$ -rays is called a doubles coincidence measurement. One involving 3  $\gamma$ -rays is called a triples coincidence measurement. At least 2 detectors are required for a doubles experiment, 3 for a triples experiment and so on. Consider a double coincidence measurement. Clearly, now 15 to 20 per cent events in each detector give useful full-energy events. Thus, in a doubles coincidence measurement, only 2 to 4 per cent of the total events obtained in the two detectors are good peak-peak values. This implies that the remaining 96 to 98 per cent events are unwanted garbage. This is a horrifying and very undesirable situation.

What is the way out of such a situation? Clearly the small peak to total ( $P/T$ ) ratio is due to the fact that the Ge-detector interacts with  $\gamma$ -rays primarily by Compton scattering in the energy range of interest. About 80 per cent events are Compton events. Is it possible to take away these Compton events from the  $\gamma$ -rays spectrum? This will increase the ( $P/T$ ) ratio. The solution is: put Compton-suppression shields around the Ge-detectors.

Figure 1.1.14 shows the outline of a Compton-suppression shield on a Ge-detector. The figure shows a  $\gamma$ -rays photon interacting with the Ge-detector.

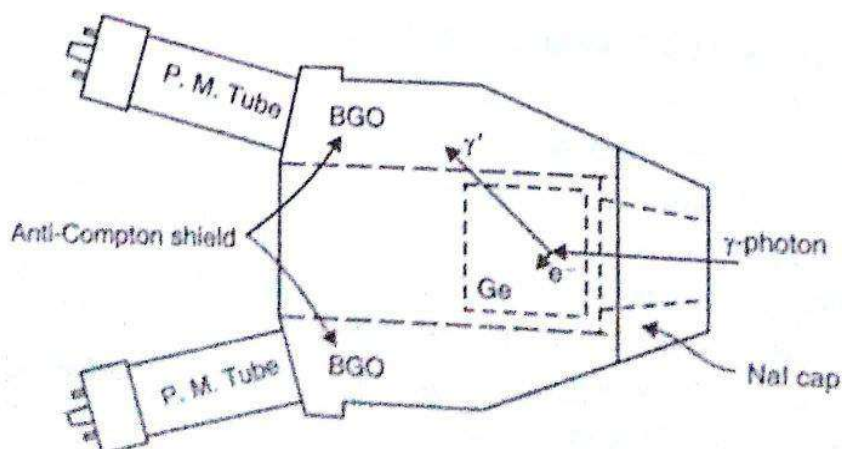


Fig. 1.1.14. Outline of the anti-Compton shield surrounding a Ge-detector. The sequence of events is discussed in the text.

The Compton scattered  $\gamma$ -photon, labelled  $\gamma'$ , is lost if there is no shield surrounding the Ge-crystal. If this shield is made from a scintillator which is sufficiently dense to stop  $\gamma'$ , then the output of the photomultiplier tube gives a signal. This signal is essentially due to the Compton events originating in the Ge-detector. By putting this pulse produced by the scintillator shield in anti-coincidence with the Ge-detector signal pulse it is possible to reject the Compton events produced in the Ge-detector. (See Sec. 1.1.6 to get an idea of about how to get a coincidence signal and an anti-coincidence signal.) This is the reason why the shield is called an anti-Compton or Compton-suppression shield. The scintillator used for such a shield has to be dense enough to stop the Compton scattered  $\gamma$ -rays. Further, its light output should be sufficiently good.

$\text{NaI}$  anti-Compton shields were successfully tried first. Large  $20 \times 25 \text{ cm}$   $\text{NaI}$  shields were placed on 6 Ge-detectors at Daresbury, University of Manchester. [P.J. Twin *et al.*, Nucl. Phys. A 409, 343 (1983)]. This gave a markedly improved ( $P/T$ ) ratio: more than 3 times the case without shielding. At Berkeley, shields of bismuth germanate (BGO) were successfully tried for the first time. This material has the chemical formula  $\text{Bi}_4 \text{Ge}_3 \text{O}_{12}$ . Its density is  $7.13 \text{ gm/cm}^3$ . In comparison, the density of  $\text{NaI}$  is only  $3.67 \text{ gm/cm}^3$ . The average atomic number  $Z$  for BGO too is higher than  $\text{NaI}$ . Consequently, this material (BGO) has a  $\gamma$ -ray absorption length 2.5 times smaller than  $\text{NaI}$ . This means more compact shields, so that more Compton-suppressed detectors can be placed near the source of  $\gamma$ -rays, usually the target kept in the path of an

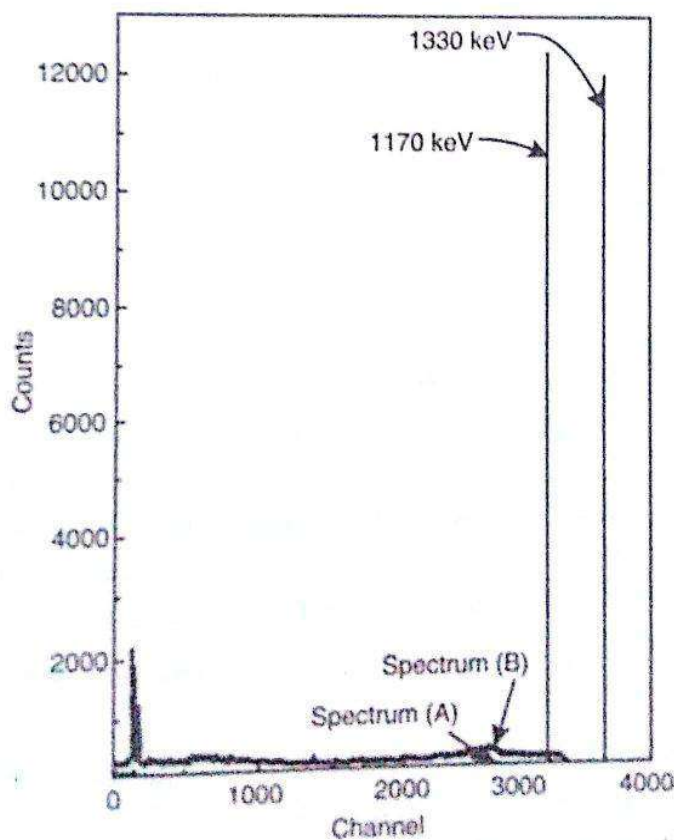


Fig. 1.1.15.  $^{60}\text{Co}$   $\gamma$ -spectrum taken with Compton-suppressed Ge (A) and an unsuppressed Ge (B). The data is without  $\text{NaI}$  cap in front of the detector. (R.M. Diamond - the Berkeley high resolution ball.)

accelerator beam. Figure 1.1.14 is the outline of the Berkeley BGO Compton-suppression shield showing a  $5 \times 5$  cm Ge-detector inside. It is actually made of six coaxially mounted BGO sections. The figure shows only two of the six photomultiplier tubes on the back surface. It also shows a NaI cap on the front, tapering portion. This NaI cap is added to suppress the  $\sim 180^\circ$  Compton scattered  $\gamma$ -rays. These  $\gamma$ -rays ( $\sim 180^\circ$ ) correspond to Compton edges just below the full-energy photo-peaks and so must be removed from the spectrum; otherwise these Compton edges appear precisely where we are interested in having a clean, low-background region in the  $\gamma$ -ray spectrum. Figure 1.1.15 shows two  $\gamma$ -rays spectra of  $^{60}\text{Co}$  taken with the Berkeley Ge-detector; one (A) with a Compton-suppressed (BGO-shielded) Ge and the other (B) with an unsuppressed Ge detector. Notice that in spectrum (A), the Compton 'hump' is almost not there. The  $P/T$  ratio now improves drastically. For spectrum (A) it is,

$$\frac{P}{T} \approx 50 - 60\%$$

For spectrum (B) it is  $\sim 15$ – $20$  per cent. The addition of NaI caps (see Fig. 1.1.14) almost wipes out any remaining Compton edge. The response function of a germanium detector can thus be seen as drastically improved.

The compactness of BGO shields has made it possible to pack as many as 21 Compton suppressed detectors at a distance of about 14 cm from the target in the system in operation at Berkeley.

Let us briefly discuss the tremendous advantage of having such an array of Compton suppressed Ge-detectors. It enables us to greatly improve the resolution of the detector—not a single detector but the system as a whole. Today Ge-detectors give the highest resolution possible about 2 keV at 1 MeV. Of course, with a single detector we cannot have more resolution. To understand this and the effect of more than one Ge-detectors, let us define resolution as the reciprocal of the number of resolvable points. Consider a range of energy 0–1 MeV and assume for the purpose of discussion, a constant resolution of 2 keV. We thus have 500 resolvable points. Two  $\gamma$ -rays falling on the same point cannot be resolved. However, in nuclear spectroscopy, we are usually not interested in single  $\gamma$ -rays but members of a  $\gamma$ -ray cascade; e.g., members of a rotational band discussed in Chapter 7. If two detectors are used, we can make use of the coincidence relationships between the two  $\gamma$ -rays (which cannot be resolved by a single detector) with the other members of their individual cascades. This is shown in Fig. 1.1.16. It is much less probable that the two pairs of  $\gamma$ -rays coincide than the original two (singles)  $\gamma$ -rays.

For two detectors in coincidence we have a two-dimensional array of points as shown in Fig. 1.1.16, bottom portion.

Notice that the 500 resolvable points of the single detector have now become  $500^2$  points in the two-dimensional array of two coincident detectors.

Coincidences of a still higher order yield more effective resolution for coincident cascades of  $\gamma$ -rays by greatly increasing the number of possible resolvable points. For instance, a triple coincidence would give us  $500^3$  possible resolvable points. So there should be as many Ge-detectors as possible close to the target.

With plain Ge-detectors, as remarked earlier, 96 to 98 per cent of the total events are unwanted garbage in a doubles coincidence measurement. With Compton-suppressed Ge-detectors, we have seen that peak to total ( $P/T$ ) ratio of over 50 per cent is obtained. In a doubles measurement therefore 50 per cent of 50 per cent i.e., 25 per cent of events are good peak-peak values. The Table 1.I.1 by R.M. Diamond (LBL preprint — 202241, Sept., 1985) shows the advantage of using Ge-detectors, it is possible to establish  $\gamma$ -cascades right up to a spin  $\sim 50 \ h$ , by

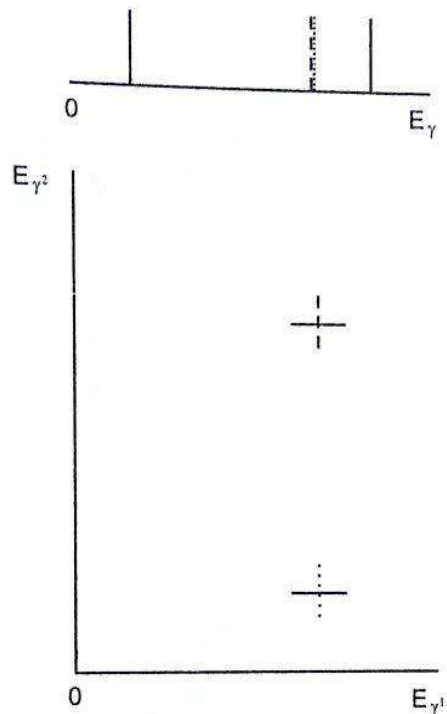


**Fig. 1.I.16.** The top portion shows how a single detector cannot resolve two  $\gamma$ -rays; they overlap. The bottom portion shows how they can be resolved in the doubles spectrum by their different cascading partners.

TABLE 1.1

<i>Type (order) of coincidences</i>	<i>Singles</i>	<i>Doubles</i>	<i>Triples</i>	<i>Quadruples</i>
	<i>Ge<sup>1</sup></i>	<i>Ge<sup>2</sup></i>	<i>Ge<sup>3</sup></i>	<i>Ge<sup>4</sup></i>
Unsuppressed Ge	20%	4%	0.8%	0.16%
Peak/Total				
Compton-suppressed	50%	25%	13%	6%
Ge Peak/Total				
Improvement factor	2.5	6	16	39

Notice that for unsuppressed Ge-detectors full-energy triple coincidences are only 0.8 per cent of the total events, making them unusable. On the other hand, the use of Compton-suppressed Ge-detector gives 13 per cent useable triples. Even quadruple coincidences can be used. Using such an array of Compton-suppressed Ge-detectors, it is possible to establish

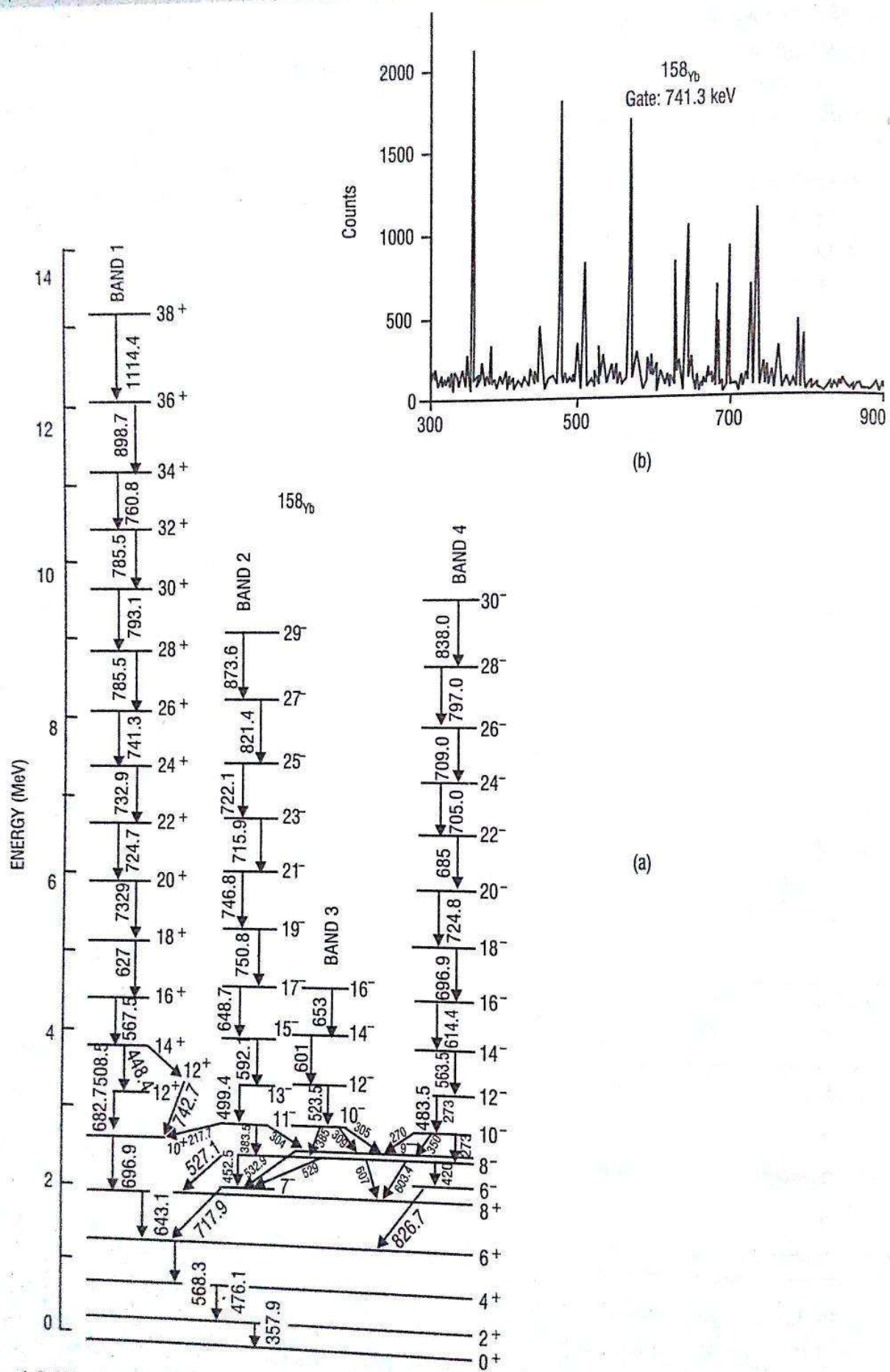


**Fig. 1.I.17.** (a) Level scheme of  $^{158}\text{Yb}$  using the Berkeley array of 21 Compton-suppressed Ge-detectors. (b) Coincidence spectrum in  $^{158}\text{Yb}$ .

$\gamma$ -cascades right up to a spin  $\sim 50 \hbar$ , by detecting  $\gamma$ -rays weakest in intensity. Multiple transitions (of the same energy) can be unambiguously placed in the energy level scheme by higher-order coincidence work. Further, nuclear spectroscopic studies at high spin are possible. In particular, this enables us to study how nuclei carry angular momentum and what are the changes that take place in shape and collective motion with the increase in spin.

Thus a new and exciting approach to nuclear structure studies opens up with the advent of Compton-suppressed Ge-detector arrays. Figure 1.I.17 (a) shows the level scheme of  $^{158}\text{Yb}$  studied by using the Berkeley array. Notice that a level with spin  $38 \hbar$  is reached. Also, many  $\gamma$ -transitions are multiple. Figure 1.I.17 (b) shows a typical coincidence spectrum in  $^{158}\text{Yb}$ . The Compton edges are practically absent.

[Ref: S.B. Patel, et al., *Phy. Rev. Lett.*, Vol. 57, 1 (1986)].

### (vi) Cloud and Bubble Chambers

Without doubt these are the most dramatic radiation detectors. The basic principle of their operation is the same: a cloud chamber contains a super-cooled vapour while a bubble chamber contains a superheated liquid. These detectors enable you to actually 'see' the path of the charged particle and the events taking place along this path. A simple expansion cloud chamber is sketched in Fig. 1.I.18. It consists of an air tight chamber having a large glass window, so that it can be illuminated and the events can be seen or photographed. The chamber contains saturated vapour of a liquid, usually water, with a little alcohol and the radioactive source. One wall of the chamber is a movable piston.

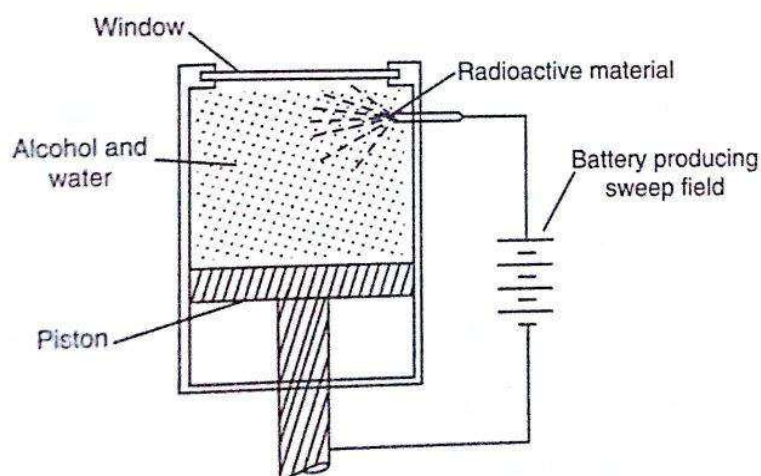


Fig. 1.I.18. Expansion cloud chamber (schematic).

If the volume of the chamber is suddenly increased by moving the piston, the adiabatic expansion results in cooling and consequent supersaturation of vapour. If there are ions within the chamber, these provide nuclei for condensation. A small electric field of few volts is provided within the cloud chamber to 'sweep out' any stray ions which are not of interest (sweep field). Clearly the chamber is sensitive for an incident charged particle, just before the piston expansion, and so the ions produced will not have enough time to get swept away and the droplets formed due to condensation will make positions of ions along the path of the particle visible. However, such a picture gets quickly spoilt as the droplets move due to gravity and gas turbulence. They

also evaporate. If the piston is then returned to its original position, it takes about a minute or so for the chamber to get ready for another expansion. By applying a magnetic field  $B$  to the chamber, the curved tracks of the incident particles can be photographed and studied. This enables one to measure the radius of curvature  $r$  and from this the velocity or energy of the incident charged particle can be computed by using the relation,

$$\frac{mv^2}{r} = qvB \quad \text{or} \quad mv = qBr \quad \dots(1.1.4)$$

The thickness of the track is characteristic of the particle. Alpha tracks can be easily distinguished from those made by electrons. On an average an  $\alpha$ -particle under atmospheric pressure produces about 50,000 ion pairs per cm in air. On the other hand,  $\beta$ -particles produce only 50 ion pairs per cm. Since both  $\alpha$ -and  $\beta$ -particles lose energy by giving up about 34 eV per ion pair produced,  $\alpha$ -tracks are *short and thick*, while  $\beta$ -tracks are *long and thin*. To the practised eye, cloud chamber tracks due to different charged particles are as different as the tracks left by different animals on wet sand. The study of cloud chamber pictures has been very rewarding and it practically enables us to 'see' reaction on an atomic scale.

When it is required to detect very *high-energy* particles, such as cosmic rays or those produced by accelerators, a *bubble chamber* is more advantageous since it is filled with a dense liquid instead of a gas. It was invented in 1952 by Glaser. In Glaser's own words: "A bubble chamber is a vessel filled with a transparent liquid which is so highly superheated that an ionising particle moving through it starts violent boiling by initiating the growth of a string of bubbles along its path."

To understand the principle of a bubble chamber consider the bottle of a carbonated soft drink like "Thums Up". Prior to the opening of the bottle, the  $\text{CO}_2$  gas over the drink and that dissolved in it are in equilibrium. When the bottle is opened, the pressure gets reduced and the solution of the gas in the liquid is supersaturated. From this unstable condition, bubbling results and we have the familiar effervescence. By adding some salt one can get a very large effervescence. Why is it so? Clearly the bubbles form most readily on discontinuities provided by the specks of salt, so that most of the  $\text{CO}_2$  gas effervesces almost at once (giving rise to much frothing). In much the same manner, when ions are produced in a bubble chamber, they act as nuclei for the formation of small bubbles.

In a bubble chamber, a superheated liquid is at a temperature and pressure lower than the equilibrium vapour pressure. This creates an unstable condition and the passage of a single charged particle initiates bubble formation. The superheated condition is thus achieved. The liquid in the chamber is first kept at the equilibrium pressure and then the pressure, like in the case of the cloud chamber, is suddenly lowered by rapidly moving a piston. A few milli-seconds after the chamber has become sensitive, the process is reversed and the chamber pressure is brought back to its equilibrium value. The time during which the chamber is sensitive is synchronised with the arrival time of the pulse of high-energy particles from an accelerator. An electronic photosflash is used to illuminate the bubbles and stereoscopic photographs are recorded. Figure 1.1.19 shows a typical bubble chamber.

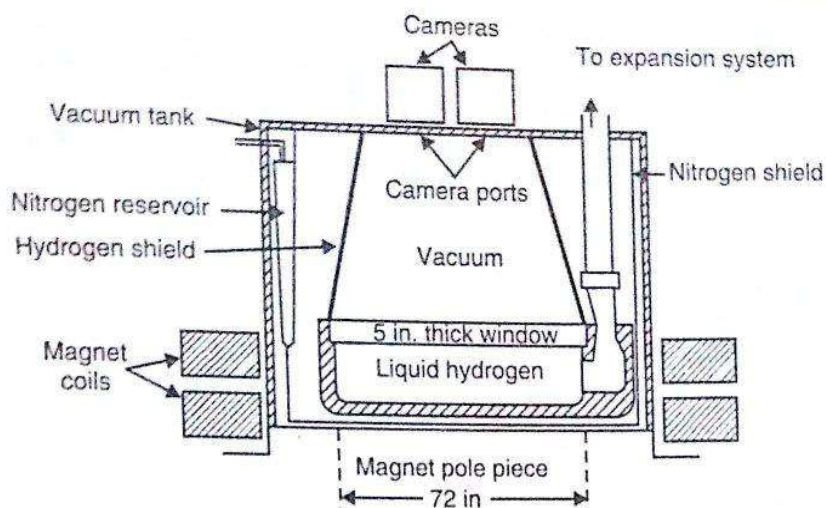


Fig. 1.I.19. A typical bubble chamber.

Glaser's first chamber contained only a few cm<sup>3</sup> of liquid. The modern bubble chambers are huge and very expensive. The superheated liquid is often hydrogen at -245°C. Sometimes xenon at -20°C or helium or deuterium is used. Extreme care has to be taken since hydrogen becomes explosive when it comes in contact with oxygen. However, hydrogen has the advantage of having the chamber function as proton target. The 12-feet hydrogen bubble chamber of the Argonne National Laboratory, USA, contains 20,000 litres of hydrogen. A superconducting magnet produces a field of about 18 kg in the chamber of volume 25 m<sup>3</sup>. Because of the high density of liquid (compared to gas) a bubble chamber is indispensable in the study of high-energy particles. The existing bubble chambers produce about 35 million photographs per year and the process of data evaluation is a complex one employing computers. In 1970, the Argonne Laboratory bubble chamber recorded the first neutrino interaction in pure hydrogen. Figure 1.I.20 schematically shows this remarkable event.

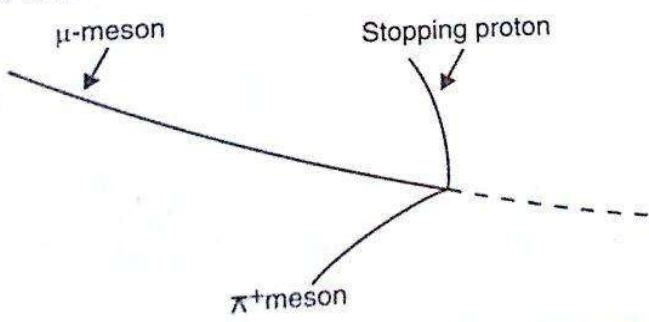


Fig. 1.I.20. Neutrino interaction in the hydrogen bubble chamber. A neutrino enters from right and interacts with the proton of hydrogen atom to yield a  $\pi^+$ , a proton and a  $\mu^-$ .

### (vii) Spark Chamber

The spark chamber is based on the simple fact that if the voltage across two metal plates separated by a distance of a few centimetres is increased beyond a certain value, a breakdown in the form of sparking occurs. [The spark chamber consists of a series of thin parallel plates spaced a few millimetres apart] as shown in Fig. 1.I.21.

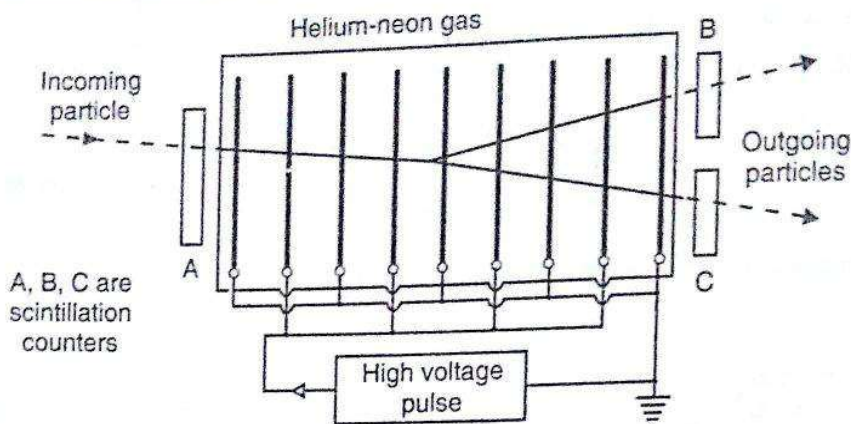


Fig. 1.I.21. Spark chamber arrangement.

The first, third, fifth and all other odd-number plates are grounded and the second, fourth, sixth and all even-number plates are connected to a high-voltage source. (A small "clearing" voltage is always operative.) [The high voltage is almost-but not quite—sufficient to produce a discharge between the adjacent plates] A 'trail' of ionisation is produced by an incident charged particle. If the voltage (in a pulse form) is applied in a fraction of a micro-second during which electrons in this 'trail' remain free (before becoming attached to molecules in the gas) a small localised spark discharge between each pair of plates will occur along the particle's path. A photograph will then reveal the trajectory of the incident particle and then collision events or deflections in a magnetic field can be observed similar to the bubble chamber. The voltage pulse is quickly removed and the ions are swept by the small field, so that the chamber is ready for the next pulse. The chief advantage of a spark chamber over a bubble chamber is that it can be made sensitive for a very short time ( $\sim 10^{-6}$  secs or so). This is because the ions remain between the plates for a few  $\mu$  sec, and so the pulse (high) voltage can be applied after passage of the particle. A spark chamber can thus be triggered.

In Fig. 1.I.21, there is one incoming particle giving rise to two charged product particles. Three scintillation counters *A*, *B* and *C* detect the three charged particles. If the particles pass through these three counters, an electronic LOGIC circuit can be made to trigger (activate) the high-voltage supply (10–20 kV). It is possible to apply this pulse within a time interval of less than 50 nano secs ( $1 \text{ ns} = 10^{-9} \text{ s}$ ), so that the resulting sparks can be photographically recorded. The track of this particular incoming particle is recorded and there is not much possibility of some *background* particle triggering off the spark track. In this way, rare events and interactions can be studied without the confusing or misleading background of unimportant events.

#### 1.1.4 PARTICLE ACCELERATORS

Nuclear detectors and accelerators are to a nuclear physicist what a microscope is to a biologist and a telescope is to an astronomer. Let us first understand the need to have accelerators for doing nuclear physics.

#### Need for an Accelerator of Charged Particles

- (a) To create a new particle or state of mass  $m$ , we need at least an energy  $E = mc^2$ . For a state of mass approximately equal to a proton, for example, we need at least an energy of about 1000 MeV.

(b) High energies are also necessary for studying the structure of nuclear systems. Let us see how.

The reduced de Broglie wavelength of a particle with momentum  $p$  is given by:

$$\lambda = \frac{\lambda}{2\pi} = \frac{\hbar}{p} \quad \dots(1.1.5)$$

where

$$\hbar = \frac{h}{2\pi}, h \text{ being Planck's constant.}$$

$$= 6.582 \times 10^{-22} \text{ MeV-sec.} \quad \dots(1.1.6)$$

We know from optics that to see the structure in detail of an object with linear dimensions  $d$ , we must use a wavelength comparable to or smaller than  $d$ .

i.e.,

$$\lambda \leq d \quad \dots(1.1.7)$$

For this wavelength, the momentum  $p$  required must then be,

$$p \geq \frac{\hbar}{d} \quad \dots(1.1.8)$$

It is clear that to see the details of very small objects like nuclear particles, high momenta and thus high energies are needed. For  $d = 10^{-15} \text{ m} = 1 \text{ fm}$ , and protons as probe, it is easy to calculate the kinetic energy required to see linear dimensions of 1 fm is about 20 MeV. Obviously, we do not have naturally produced beams of particles with such energies; they must be produced artificially.

Today we have accelerators producing beams of charged particles with energies ranging from a few MeV to giant machines giving a few hundred GeV ( $1 \text{ MeV} = 10^6 \text{ eV}$ ,  $1 \text{ GeV} = 10^9 \text{ eV}$ ). Intensities can be as high as  $10^{16}$  particles per sec. The beams can be concentrated on targets of only a few  $\text{mm}^2$  in area. The particles that are most often used as *projectiles* are protons and electrons.

Let us now consider in brief the principles of some widely used accelerators.

### (i) Van de Graaff Generator

This electrostatic generator was first built by Van de Graaff in 1931. In this generator, a charge  $Q$  is transported to one terminal of a huge condenser  $C$ . This results in a voltage

$$V = \frac{Q}{C},$$

which is used to accelerate the ions. Figure 1.1.22 shows the main features of a Van de Graaff accelerator. A voltage of 30 kV is used to spray positive charges on an insulating belt made of rubber, silk, linen or paper. This belt is motor-driven to carry the charge continuously to the dome-shaped terminal, where it is removed. To spray and collect charges, sharp spray-points.

called *corona points* and *collector points* respectively, are used. Positive ions are produced in the ion source. These are usually protons, deuterons,  $\alpha$ -particles. They are accelerated in the evacuated accelerating

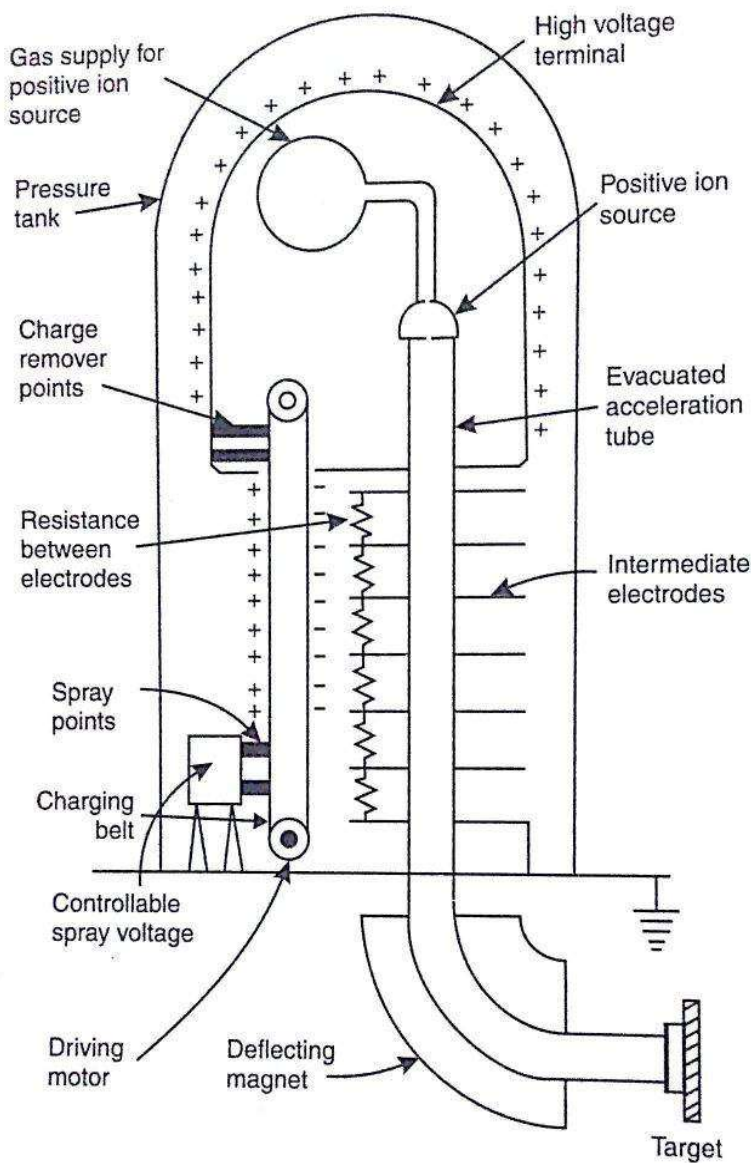


Fig. 1.I.22. Schematic diagram of a Van de Graaff accelerator.

tube. When this system is placed in air, voltages of up to a few MeV can be reached, beyond which the insulation provided by air breaks down. If the system is placed in a pressure tank filled with an inert gas like nitrogen and carbon dioxide (~5 per cent) at pressure 15 atm., voltages up to 12 MV and current, up to about  $100 \mu$  amperes can be obtained. (At higher pressures, air can withstand stronger electric fields before breakdown occurs.)

The Tandem Van de Graaff accelerator is an ingenious modification of the Van de Graaff generator. Here two insulating columns are used back-to-back in one pressure tank, so that the particles are accelerated to energies twice the energies given by the conventional Van de Graaff machine.

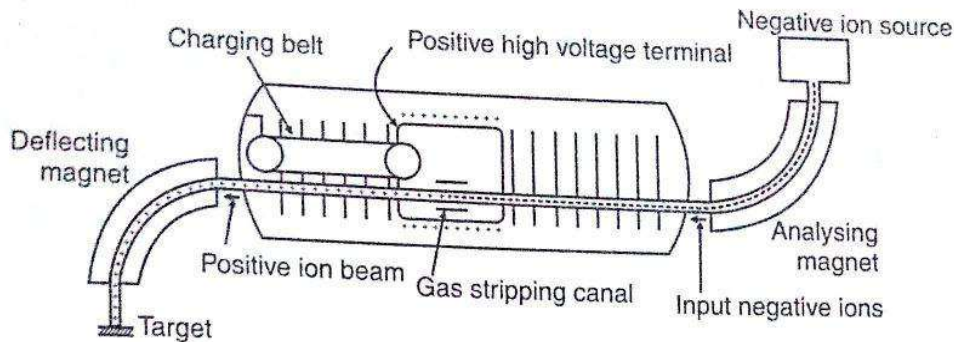


Fig. 1.I.23. Tandem Van de Graaff accelerator.

Figure 1.I.23 schematically shows the Tandem Van de Graaff accelerator. Note that the terminal (high, positive voltage) is in the middle of a long pressure tank and the ion source producing negative ions like  $H^-$  is at one end. These negative ions get accelerated towards the central positive terminal, where they enter a gas-containing canal, called *stripping canal*. Here the negative ions are stripped of their electrons and become positive ions. The positive ions are repelled from the positive terminal and go on gaining energy as they go to the grounded region to hit the target. The total energy gain is therefore twice that of a single-stage Van de Graaff machine. About 30 MeV protons can be obtained by Tandem Van de Graaff generator.

## (ii) The Cyclotron

It is another commonly employed machine for producing high-energy particles, first developed by E.O. Lawrence and M.S. Livingston in 1931. Figure 1.I.24 schematically shows the path of a charged particle in a cyclotron.

A short hollow, cylinder is divided into two ‘dees’— $D_1$  and  $D_2$  resembling the letter D. These dees are placed between the poles of a large electromagnet (Poles of  $\sim 5$  ft diameter), so that the magnetic field is parallel to the axis of the cylinder. (Of course, the dees have to be kept in a vacuum chamber, which in turn is to be kept between the magnetic poles.) An ion source is kept at the centre between the dees (usually giving protons). The two dees— $D_1$  and  $D_2$  are connected to the terminals of a high-frequency oscillating (A.C.) circuit. This changes the charge on each dee several million times per second. When  $D_1$  is negative, protons are attracted towards it. Inside  $D_1$ , the magnetic field  $B$  makes each proton travel in a circle of radius  $r$ , given by:

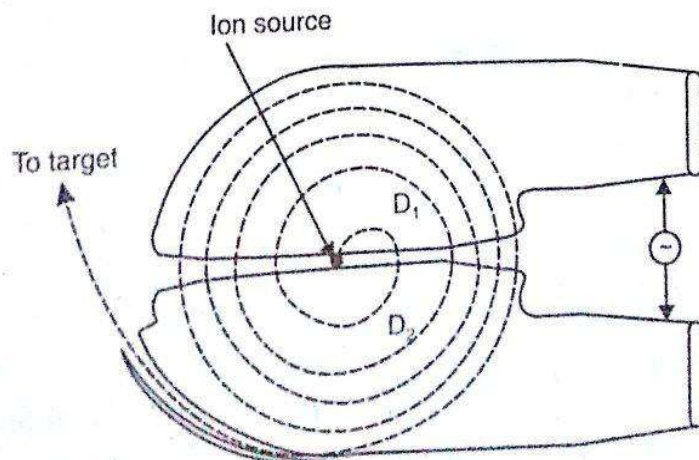


Fig. 1.I.24. Path of a charged particle in a cyclotron.

$$\frac{Mv^2}{r} = Bqv \quad \dots(1.1.9)$$

where  $M$  and  $q$  are mass and charge of the proton. Once inside the dee, the protons (or any other charged particles) are in an *electric field-free zone* and as a result, move with constant speed. After travelling one semicircle, the proton comes to the edge of  $D_1$ . If we now adjust the frequency of the oscillator is such a way that by the time the proton comes to the edge of  $D_1$ , the potential difference between  $D_1$  and  $D_2$  changes direction so as to make  $D_2$  negative and  $D_1$  positive. The proton will then get attracted to  $D_2$  and its speed will increase due to the acceleration. Once inside  $D_2$ , the proton is in a field-free zone again and it will now move in a circular path at constant speed (higher than the previous constant speed in  $D_1$ ). The radius of the path in  $D_2$  will be larger. After traversing a semicircle in  $D_2$ , the proton will come at the edge of  $D_2$ , where, if the direction of the electric field changes, it will receive additional energy. The proton will continue travelling in semicircles of increasing radii every time it goes from  $D_1$  to  $D_2$  and from  $D_2$  to  $D_1$ .

[The important fact is that the time required by the proton to travel a semicircle (within the dee) is independent of the radius of the circle.]

Let us verify this. If  $t$  is the time required to travel a distance  $\pi r$  (semicircle) with speed  $v$ ,

$$t = \frac{\pi r}{v}$$

From Eq. 1.1.9,

$$v = \frac{Bqr}{M}$$

$$t = \frac{\pi r}{\frac{Bqr}{M}} = \frac{\pi M}{Bq}$$

... (1.1.10)

[Thus by adjusting the magnetic field  $B$ ,  $t$  can be made the same as that required to change the potentials of  $D_1$  and  $D_2$ .]

Protons gain tremendous energy after traversing through several rotations. When they come near the circumference of the 'dees', an auxiliary electric field is used to deflect them from the circular path to eventually reach a target.

[The voltage between  $D_1$  and  $D_2$  is usually 100,000 volts.] When a particle emerges from the cyclotron, due to successive accelerations it acquires an energy of tens of MeV. Thus a comparatively low voltage is used to get high-energy particles. [The upper limit of energy for a proton is about 22 MeV. This is because, Eq. 1.1.9 is non-relativistic and as the speed of the particle increases its mass increases too.] This disturbs the cyclotron operation—the speed does not increase at the proper rate so as to remain in phase with the oscillations.

To get some idea of how large the frequency might be, let us calculate it, for proton and a magnetic field of 1 Wb/m<sup>2</sup> or 10,000 gauss.

$$\text{Frequency } f = \frac{\omega}{2\pi} = \frac{v}{2\pi r} = \frac{Bq}{2\pi M} \quad (\text{from Eq. 1.I.10})$$

$$= \frac{1 \text{ Wb/m}^2 \times 1.6 \times 10^{-19} \text{ coul.}}{2 \times 3.14 \times 1.67 \times 10^{-27} \text{ kg}} = 1.52 \times 10^7 \frac{\text{cycles}}{\text{sec}}$$

$$= 15.2 \frac{\text{megacycles}}{\text{sec}} \quad \text{or} \quad 15.2 \text{ MHz}$$

In other words, a radiofrequency source is required.

### (iii) Synchrotron

The cyclotron Eqs. 1.I.9 and 1.I.10 are non-relativistic. As the mass of the particle increases,  $B$  also should be increased to satisfy Eq. 1.I.10. For non-relativistic velocities, K.E. of particles in a cyclotron is,

$$\text{K.E.} = \frac{1}{2} Mv^2 = \frac{1}{2} \frac{B^2 r^2 q^2}{M} = Vq \quad \dots(1.I.11)$$

where,  $V$  is the effective potential difference through which the particles have been accelerated.

$$V = \frac{1}{2} B^2 r^2 \frac{q}{M} \quad \dots(1.I.12)$$

It is clear from Eq. 1.I.12 that the energy increases as the square of both  $B$  and  $r$ . As the mass increases for a fixed  $B$  and  $q$ , the required frequency goes down and as a result, the particles in a fixed frequency machine go 'out of step' with the accelerating voltage.

Figure 1.I.25 illustrates another important requirement for the cyclotron if the particles are to be kept together in a beam. [The magnetic field must be shaped so that if a particle moves vertically away from a central plane, it experiences a restoring force.] To accomplish this, the magnetic force field should get weaker as the radius increases. This is shown by curved lines of force in Fig. 1.I.25. The force experienced by the particles above and below the central plane is also indicated.

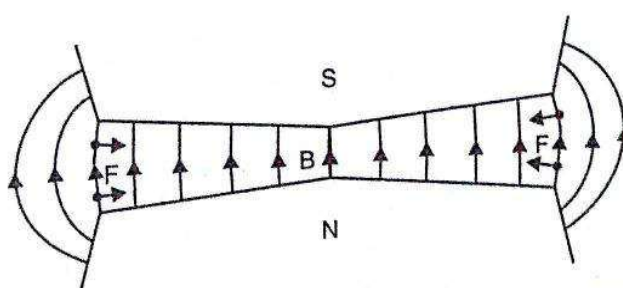


Fig. 1.I.25. This magnetic field produces vertical focussing in a cyclotron. The particles move in a plane perpendicular to  $\vec{B}$ .

Thus the vertical focusing requirement implies that the field must decrease with the radius, which is just the opposite of the variation required to compensate for a relativistic increase in mass. It is obvious from Eq. 1.1.9 that as  $M$ , increases, the frequency  $\omega (\equiv v/r)$  can remain constant only if  $B$  increases to keep the ratio of  $B$  to  $M$  constant. It turns out that this approach conflicts with the focusing conditions of the beam. Relativity sets a limit to the maximum energy that can be obtained using a cyclotron, which for protons is about 22 MeV.

To reach higher energies, Veksler and independently, McMillan suggested an ingenious technique in 1945 which uses the principle of *phase stability*. Let us understand this principle somewhat qualitatively as a full picture is beyond the scope of this book.

### Phase Stability and Phase Oscillations

Consider a particle circulating in an orbit through a constant magnetic field and crossing a gap (between the dees) with an applied alternating electric field. Let us assume that the velocity of the particle is such as to make it cross the gap when the electric field is zero. The particle will then circulate in this orbit at a constant velocity. The energy, frequency and radius of this orbit are referred to as *synchronous* and the particle is called synchronous particle.

Suppose now that another particle arrives at the gap a little earlier (at time  $t_1$ ) than a synchronous particle. This is shown in Fig. 1.1.26. This particle will clearly gain energy in crossing the gap. Because of this gain in energy, its angular frequency will decrease ( $\omega = Bq/M$  and so an increase in  $M$  implies a decrease in  $\omega$ ) and the particle will next cross the gap at a time  $t_2$ , which is closer to the moment the synchronous particle crosses the gap. This process continues and each time the particle comes a little closer in phase to the synchronous particle ( $t_2, t_3, \dots$ ). When it crosses the gap in phase with the synchronous particle, there is no electric field. However, the energy of the particle by now is higher than the synchronous particle and so after some turns, it enters the decelerating part of the cycle. In this part, the particle loses energy and hence its angular frequency  $\omega$  increases. It is back in phase with the synchronous particle. Thus the phase energy and radius of the orbit of a particle oscillate around the equilibrium situation of a synchronous particle.

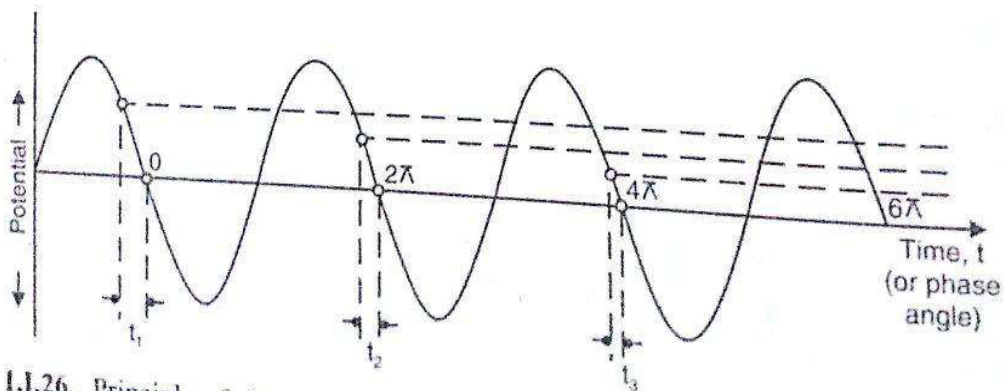


Fig. 1.1.26. Principle of phase stability.  $O$  corresponds to the synchronous particle.

A group of particles therefore can be carried out to the maximum possible radius in a series of phase stable, synchronous orbits, by starting with a frequency  $\omega_0 = Bq/m_0$  and then slowly

decrea  
the pl  
decre  
with i  
can a  
the m  
arour  
oscill  
incre

1  
radit  
keep  
of a

(i  
T  
tl  
n  
f  
c  
1  
1

decreasing the frequency. Note that the smaller  $\omega$  is made, the larger becomes the radius of the phase stable orbit. In other words, by keeping the magnetic field constant and slowly decreasing the frequency of the accelerating field, the radius of the orbit would increase along with the energy of the bunch of particles. This is the principle of the *synchrocyclotron*. We can also increase the magnetic field very slowly, keeping the frequency constant. In this case the momentum (and so energy) of the bunch of particles increases as the radius oscillates slightly around the equilibrium value. This is the principle of the *synchrotron*. In each case, the energy oscillates around the equilibrium value (corresponding to the synchronous orbit), which slowly increases with time.

The advantage of synchrotron over synchrocyclotron is obvious. The synchrotron is a constant radius machine. The ions move in an evacuated ring to which a magnetic field is applied to keep the charged particle in an orbit of proper radius. Figure 1.I.27 shows the essential features of a synchrotron. For the sake of simplicity only a few of the repetitive elements are shown.

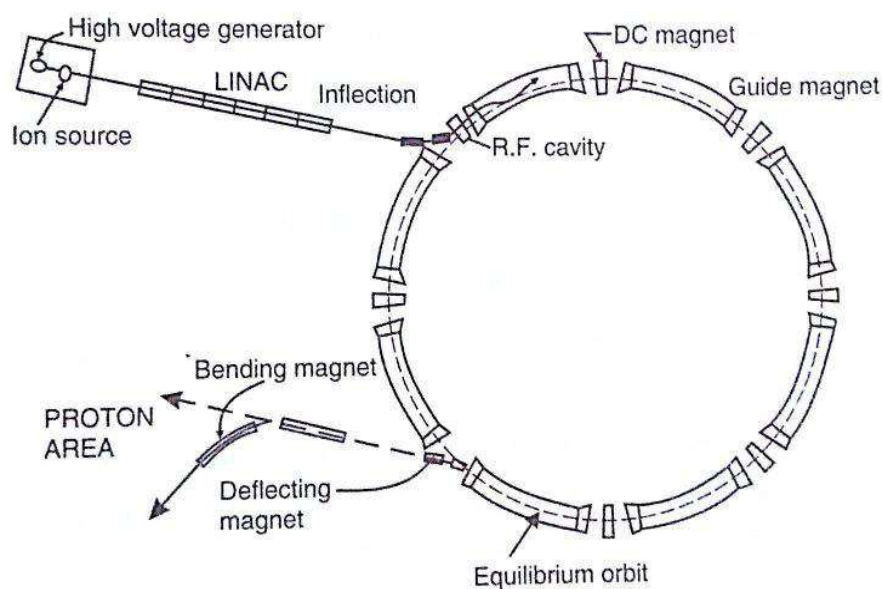


Fig. 1.I.27. Features of a proton synchrotron.

#### (iv) The Betatron

The betatron is an electron accelerator which uses the principle of electromagnetic induction as the accelerating force. Electron moving in a circular annular vacuum chamber under a guiding magnetic field are accelerated by a magnetic flux time varying linking the electron's orbit. The first successful machine was built by D.W. Kerst in 1940. In the betatron, the rate of increase of the flux linking the electron's orbit is very slow compared to the circulation frequency. The electrons are accelerated continuously during the beginning of the rising magnetic field (see Fig. 1.I.29). To ensure that the electrons are held on a fixed orbit of radius  $r_0$ , a certain relation between the flux density at the orbit  $B_0$  and the total flux linking the whole orbit must be satisfied. This relation is easily derived.